# The light-activated signaling pathway in SCN-projecting rat retinal ganglion cells

Erin J. Warren,[1,2] Charles N. Allen,[1] R. Lane Brown[3] and David W. Robinson[1]

[1]Center for Research on Occupational and Environmental Toxicology, L606, Oregon Health & Science University, 3181 SW Sam Jackson Park Road, Portland, OR 97239, USA
[2]Neuroscience Graduate Program and
[3]Neurological Sciences Institute, Oregon Health & Science University, 505 NW 185th Avenue, Beaverton, OR 97006, USA

## Abstract

In mammals, the master circadian clock resides in the suprachiasmatic nuclei (SCN) of the hypothalamus. The period and phase of the circadian pacemaker are calibrated by direct photic input from retinal ganglion cells (RGCs). SCN-projecting RGCs respond to light in the absence of rod- and cone-driven synaptic input, a property for which they are termed intrinsically photosensitive. In SCN-projecting RGCs, light activates a nonselective cationic current that displays inward and outward rectification. The goal of the present study was to investigate the identity of the light-activated ion channel and the intracellular signaling pathway leading to its activation. We considered two candidate channels, cyclic nucleotide-gated (CNG) channels and transient receptor potential (TRP) channels, which mediate vertebrate and invertebrate phototransduction, respectively. We report that the intrinsic light response relies upon a G-protein-dependent process. Although our data indicate that cyclic nucleotides modulate the signaling pathway, CNG channels do not appear to conduct the light-activated current because (i) cyclic nucleotides in the pipette solution do not activate a conductance or completely block the light response, (ii) CNG channel blockers fail to inhibit the light response, (iii) the effects of internal and external divalent cations are inconsistent with their effects on CNG channels, and (iv) immunohistochemistry reveals no CNG channels in SCN-projecting RGCs. Finally, we show that the pharmacology of the light-activated channel resembles that of some TRPC channel family members; the response is blocked by lanthanides and ruthenium red and SK&F 96365, and is enhanced by flufenamic acid and 1-oleoyl-2-acetyl-*sn*-glycerol. Furthermore, immunohistochemical experiments reveal that TRPC6 is expressed in many RGCs, including those that express melanopsin.

## Introduction

In mammals, the master circadian clock resides in the suprachiasmatic nuclei (SCN) of the hypothalamus (Moore & Eichler, 1972; Moore, 1983). The period and phase of the circadian clock are calibrated by direct photic input from retinal ganglion cells (RGCs) that constitute 1–2% of the total RGC population (Moore *et al.*, 1995; Gooley *et al.*, 2001; Morin *et al.*, 2003; Sollars *et al.*, 2003). SCN-projecting RGCs respond to light in the absence of rod- and cone-driven synaptic input, a property for which they are termed intrinsically photosensitive (Berson *et al.*, 2002; Hattar *et al.*, 2002). In previous work, we have shown that light stimulation triggers a slowly activating inward current in these neurons (Warren *et al.*, 2003). The response is coincident with an increase in membrane noise fluctuations, suggesting that light causes ion channels to open. Current-clamp recordings reveal that a slow depolarization, which drives low-frequency action potentials, underlies the intrinsic light response (Berson *et al.*, 2002; Warren *et al.*, 2003).

The goal of this study was to investigate the identity of the light-activated ion channel and the intracellular signaling pathway that leads to its activation in SCN-projecting RGCs. Cyclic nucleotide-gated (CNG) channels and transient receptor potential (TRP) channels were considered candidates for the light-activated channel. CNG channels

mediate a hyperpolarizing light response in the vertebrate rod and cone photoreceptors (Fesenko *et al.*, 1985; Baylor, 1987). Via activation of the G-protein transducin and a cGMP-dependent phosphodiesterase, light causes a decrease in the cytosolic concentration of cyclic GMP. In response, CNG channels in the plasma membrane close, causing a reduction in the tonic inward cationic current and a decrease in the open channel noise (McNaughton, 1990). By contrast, the TRP channel family, which was first identified in the *Drosophila* photoreceptor, mediates sensory transduction in several invertebrate species (Hardie & Minke, 1992; Montell, 2003; Bandyopadhyay & Payne, 2004). In *Drosophila* photoreceptors, light stimulation increases internal concentrations of diacylglycerol and inositol 1,4,5-trisphosphate ($IP_3$) through a $G_{q/11}$-phospholipase C-coupled cascade. The consequent activation of an inward cationic current mediated by TRP channels causes an increase in channel noise and depolarization of the photoreceptor cell membrane (Hardie, 2001). Our data support a role for TRP channels, but not CNG channels, in the intrinsic light response of SCN-projecting RGCs.

## Methods

### Stereotaxic injection of fluorescent retrograde tracer

Surgical procedures were carried out in compliance with guidelines from the National Institutes of Health, and in accordance with protocols approved by the Institutional Animal Care and Use

*Correspondence*: Dr D. W. Robinson, as above.
E-mail: robinsda@ohsu.edu

Committee of Oregon Health & Science University. Because retinas from younger rats were more amenable to patch-clamp recording, we used 6-week-old Sprague–Dawley rats, weighing between 120 and 170 g (Charles River, Wilmington, MA, USA). Tetramethyl-rhodamine-dextran (3000 mol. wt; 10 mg∕mL; Molecular Probes, Eugene, OR, USA) was injected into the SCN using a stereotaxic apparatus (Cartesian Designs, Inc., Sandy, OR, USA) to enable unequivocal identification of RGCs projecting to the circadian system (Warren *et al.*, 2003). Animals were anesthetized by i.p. injection of a solution containing Ketamine, xylazine, and acepromazine. Between 2 and 10 days after injection, animals were killed by cervical dislocation following deep anesthesia with ether.

### Electrophysiology

The anterior chamber of each eye was removed, and the retinas were gently peeled from the eyecup under a Leica GZ4 dissection scope and stored in oxygenated EMEM (HEPES modification) at room temperature. A small piece of retina was mounted on nitrocellulose filter paper containing a 2-mm hole that provided access for the recording electrode. This preparation was placed in the recording chamber on a Zeiss Axioscope 2 FS microscope with the ganglion cell layer facing up. SCN-projecting RGCs were identified by the presence of fluorescent tetramethylrhodamine-dextran using epifluorescent illumination.

Patch pipettes with tip resistances between 3 and 8 MΩ were fabricated from filamented borosilicate glass (OD 1.5 mm, ID 0.86 mm) using a P-97 electrode puller (Sutter Instruments, Novato, CA). Recordings were made at 22 °C with a Multiclamp 700A amplifier controlled by pClamp9 software via a Digidata 1320 interface (Axon Instruments, Hayward, CA, USA). During voltage-clamp recordings, cells were held at −60 mV. Series resistance was noted but uncompensated. Data were low-pass filtered at rates between 2 (voltage-clamp) and 5 (current-clamp) kHz and digitized at rates between 2.5 and 10 kHz.

For voltage-clamp whole-cell recordings, recording electrodes were filled with an intracellular solution containing (in mM): 121 KCl, 1 $MgCl_2$, 10 HEPES, 10 EGTA, 4 Mg-ATP, 0.3 $Na_3$-GTP, 2 creatine phosphate (Na salt), Lucifer Yellow (0.1%) at pH 7.35 (290 mOsm). When 18 mM K-BAPTA was used in calcium buffering experiments, KCl was reduced to 77 mM. For current-clamp perforated-patch recordings, electrodes were filled with an intracellular solution containing (in mM): 117 KCl, 10 HEPES, 10 EGTA, 4.0 Mg-ATP, 0.3 $Na_3$-GTP, 2 creatine phosphate (Na salt), Lucifer Yellow, 0.1%, Nystatin, 3 mg∕mL, pH 7.35 (290 mOsm). Adequate perforation was determined by monitoring input resistance throughout the experiment. In all experiments, the bath solution consisted of (in mM): 127 NaCl, 7 KCl, 3 $CaCl_2$, 1 $MgCl_2$ and 10 HEPES, 10 D-glucose, pH 7.4 (290–300 mOsm), and was continuously bubbled with oxygen.

Drugs were purchased from Sigma-Aldrich.

### Light stimulation

Illumination was provided by a 250-W tungsten–halogen light source through the transmitted light path of a Zeiss Axioscope 2 FS microscope, and the intensity was reduced using a variety of neutral density filters. Light intensities were determined using a radiometer (International Light, Newburyport, MA, USA). All recordings were conducted in a dimly lit room exposing the retina to 0.5 µW∕$cm^2$ of background illumination. The retinal dissection was performed under about 100 µW∕$cm^2$ white light. Following dissection, retinas were

recovered in oxygenated EMEM under dim background light for 1–6 h before recordings were begun. Intrinsic responses were elicited by exposure to 140 µW∕$cm^2$ white light. Infrared illumination was used to visualize the tissue during electrode placement so as not to elicit a light response immediately prior to recording.

### Antibodies

Polyclonal antibodies directed against the carboxy-terminal peptide of rat melanopsin (KPTKTRHLPSLDRRM) were generated in rabbits following conjugation to KLH via an amino-terminal cysteine (SigmaGenosys). Melanopsin-specific antibodies were purified by affinity chromatography on a column containing the immunizing peptide coupled to SulfoLink Gel (Pierce, Rockland, IL, USA). The monoclonal antibody (PMc 1D1) directed against CNGA1, the primary subunit of the rod photoreceptor CNG channel, was the gift of Dr Robert S. Molday [University of British Columbia (Wassle *et al.*, 1992)]. Monoclonal antibodies CRO2H7 against CNGA2 from olfactory receptor neurons, and CNC9C1 against CNGA3 from cone photoreceptors, were gifts of Dr U. Benjamin Kaupp [Forschungs-zentrum, Julich, Germany; (Meyer *et al.*, 2000)]. Affinity-purified rabbit anti-TRPC6 polyclonal antibodies were the generous gift of Dr Yasuo Mori [Kyushu University, Fukuoka, Japan; (Inoue *et al.*, 2001)].

### Immunohistochemistry

Retinas were isolated using the techniques described above and fixed in PBS containing 4% paraformaldehyde at 4 °C for 1 h. Following cryoprotection in 30% sucrose, the retinas were immersed in OCT media (TissueTech) and flash frozen. Twenty-micrometre-thick vertical sections were cut on a cryostat and thaw-mounted onto Superfrost slides (Fisher Scientific).

For double labeling of melanopsin and CNG channel subunits, sections were blocked in 1% BSA, 5% normal goat serum and 0.5% Triton-X100 for 1 h at 25 °C, and then incubated for 2 h in primary antibodies: α-melanopsin (0.5 µg∕mL); and either α-CNGA1 (1 : 100 dilution of ascites fluid), α-CNGA2 (1 : 200) or α-CNGA3 (1 : 25). After washing with PBS, a mixture of secondary antibodies was applied for 1 h at 25 °C (1 µg∕mL Alexa488-labeled goat α-rabbit IgG and 1 µg∕mL Alexa594-labeled goat α-mouse IgG, Molecular Probes). Sections were then rinsed in PBS and mounted in Slowfade Light with DAPI (Molecular Probes).

The antibodies against melanopsin and TRPC6 were both raised in rabbits. Therefore, we used a tyramide signal amplification (TSA) technique to enable reliable double immunostaining. Sections were blocked for 1 h using a 1% solution of the Blocking Reagent (TSA kit #12, Molecular Probes). Primary antibodies against melanopsin were diluted to 0.05 µg∕mL; at this dilution there was no detectable labeling of melanopsin under the standard conditions described above. After 2 h incubation in α-melanopsin antibodies, sections were washed in PBS, and incubated with 5 µg∕mL HRP-conjugated goat α-rabbit IgG for 1 h. A 1 : 100 dilution of the Alexa488-tyramide solution was then applied for 15 min in the Amplification Buffer, which contained 0.0015% $H_2O_2$. Following washing in PBS the sections were blocked with PBS containing 1% BSA and 10 µg∕mL goat α-rabbit Fab fragments (Jackson ImmunoLabs, West Grove, PA, USA). Next, a 1 : 1000 dilution of α-TRPC6 antibodies was applied for 2 h. The sections were then washed in PBS and incubated with Alexa594-labeled goat α-rabbit IgG secondary antibodies. After washing, the sections were coverslipped as described above.

### Microscopy

Images were acquired on a Zeiss LSM510 confocal microscope using 488-nm and 543-nm laser lines and the appropriate filter sets. Z-sections were taken at 0.5–1.0 μm focal planes, and a projection image was created using Metamorph software. Contrast and brightness were optimized using Adobe Photoshop 7.0.

### Statistics

Averages are reported as the mean ± SEM. Significance was determined using the Student's $t$-test. Variance between groups was determined using one-way ANOVA.

## Results

### Light response of SCN-projecting RGCs in voltage-clamp

All responses recorded in voltage-clamp to date were similar to the response shown in Fig. 1A: light (bar) stimulation triggers a slowly activating inward cationic current in the ganglion cell. The increase in membrane noise during the response suggests that ion channels are opening rather than closing. The rate at which the response decays to baseline and the extent of decay during the light stimulus depended upon the length of the light stimulus and on the individual cell.
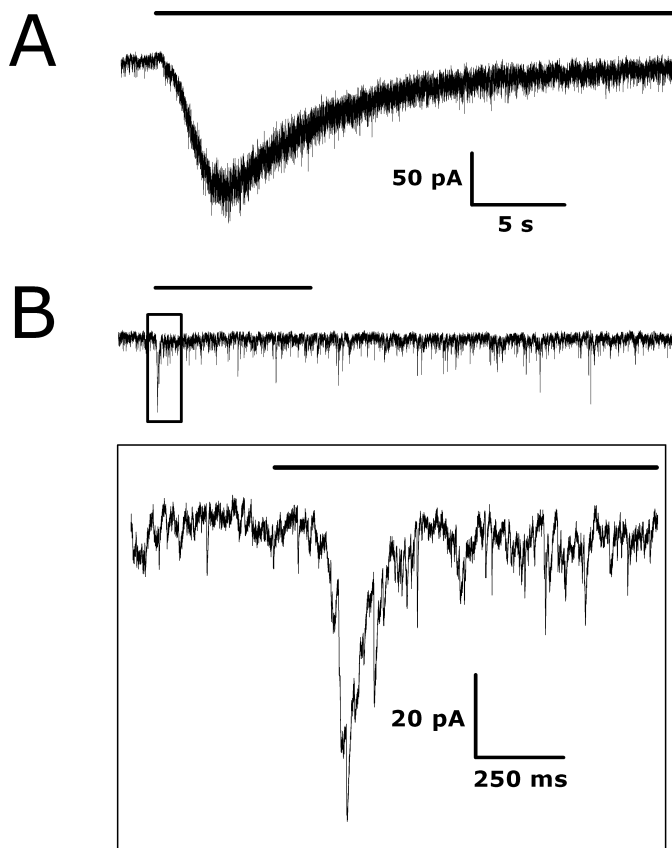


**A**

50 pA

5 s

**B**

20 pA

250 ms

FIG. 1. Intrinsic and synaptically driven light responses from RGCs held at −60 mV. (A) Whole-cell voltage-clamp recording of an intrinsic light response recorded from an SCN-projecting RGC. (B) Upper panel depicts a synaptic light response from a non-SCN-projecting Type I RGC plotted on the same time scale as the trace in A. The box is expanded in the lower panel to show an increase in synaptic currents following the onset of light. Black bars represent light stimulation.

Differences exist, both in time course and in shape, between the light responses of SCN-projecting RGCs (Fig. 1A) and the synaptically driven light responses of other ganglion cells (Fig. 1B). For example, the response of the Type I ganglion cell depicted in Fig. 1B exhibited a transient burst of synaptic activity that took 220 ms to reach peak amplitude and persisted for only 420 ms following light stimulation. By contrast, the intrinsic light response evoked in Fig. 1A required 3.3 s to reach peak amplitude and persisted for 12.7 s before decaying to a plateau. The interval between the light flash and the onset of the intrinsic response in SCN-projecting RGCs depends on the flash intensity, and can range from 200 ms in bright light to over 2 s in very dim light. The marked differences in time course make it extremely easy to distinguish between the intrinsic light responses of SCN-projecting RGCs and those generated by synaptic activity driven by rods and cones. Also noteworthy is the relative quiescence of SCN-projecting RGCs, which exhibit very little synaptic activity at rest.

Rundown of the light-activated current in SCN-projecting RGCs can be quite marked during whole-cell patch-clamp recordings, and internal solutions were selected which maximize and stabilize the amplitude of the light-activated current. As shown by the top curve (squares) in Fig. 2C, average rundown of the light-activated current within the first 20 min of recording was 45.4 ± 7% ($n = 5$) under control conditions. The response amplitude did not rundown to zero, but instead reached steady-state amplitude. Drug application via the bath solution commenced only after a steady-state response was obtained to ensure that subsequent current reduction was an effect of drug application and not response rundown.

### Role of G proteins

The slow activation and inactivation kinetics, as well as the subsequent rundown, of the light-induced current in SCN-projecting RGCs during whole-cell recordings suggest that channel activation lies downstream of an intracellular second messenger system. Phototransduction via CNG channels in vertebrates, and TRP channels in invertebrates, is coupled to transducin and $G_{q/11}$, respectively. We investigated first whether the intrinsic light response is G-protein dependent. If so, we hypothesized that inclusion of the nonhydrolysable stimulatory GTP analog, GTPγS (300 μM), in the pipette solution would constitutively activate the ion channel in question and block subsequent light responses. On average, GTPγS decreased the light response by 92 ± 6% ($n = 4$, $P = 0.008$) and the average time required for maximal effect was 20 ± 4 min (Fig. 2C). Within the first 4 min of recording, the average reduction in response amplitude was 50 ± 10%. Our finding that the baseline membrane current did not shift to that of the initial light response amplitude indicates that constitutive activation of all G-proteins leads to inactivation or desensitization of the light-activated channel.

Substitution of GDPβS, a competitive inhibitor of GTP binding, for intracellular GTP inhibits G-protein-dependent processes. If the intrinsic light response is G-protein dependent, infusion of 1 mM GDPβS in the pipette should block the light response. The average decrease in amplitude was 89 ± 5% ($n = 4$, $P = 0.006$) and the average time required for maximal effect was 25 ± 4 min (Fig. 2C). Within the first 4 min of recording, the average reduction in response amplitude was 48 ± 18% (Fig. 2C).

The reduction of the light response with GTP analogs in the pipette is quantitatively different from the reduction caused by rundown under control conditions (Fig. 2C). First, light responses were nearly abolished in the presence of GDPβS and GTPγS with only an average of 11% and 8% of maximum, respectively, persisting. By contrast, control cells reached a steady state at ~ 40% of maximum. Secondly,
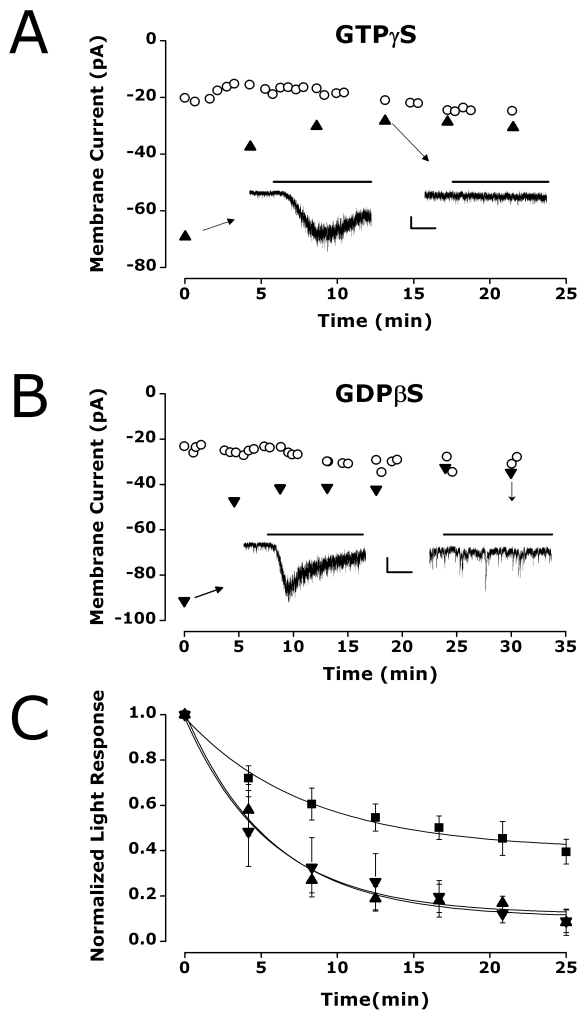
FIG. 2. The intrinsic light response is G-protein dependent. Whole-cell baseline currents were sampled throughout the recordings (○). Triangles represent the peak of the light-activated currents. Inset traces show light responses before (left) and after (right) block of response. Scale bars: 2 s, 20 pA; bar represents light stimulation. (A) In one SCN-projecting RGC, 300 μM GTPγS (▲) caused a 55% reduction in the amplitude of the light response between the first light stimulus and a second light stimulus delivered 4 min later. The amplitudes of responses elicited by subsequent steps of light were reduced by 91%. (B) In one SCN-projecting RGC, 1 mM GDPβS (▼) in the recording pipette reduced the light response by 96%. (C) Normalized group data from seven control cells containing 300 μM GTP (■) is plotted alongside normalized data from cells containing GTPγS (▲; $n = 4$) and GDPβS (▼; $n = 4$).

the reduction in the amplitude of the light response occurred faster in the presence of GTP analogs. On average, the amplitude of the light response in control cells declined to 50% of the initial value in 20 min, while the amplitude diminished to the same level in only 4 min in the presence of GTPγS and GDPβS.

## Potential role of CNG channels

CNG channels were considered as possible mediators of the light-activated current because of their central role in vertebrate rod and cone phototransduction. If cyclic nucleotides directly gate the light-activated ion channel, then their inclusion in the pipette solution should have two consequences: an inward current should develop as

CNG channels open, and eventually the light response should be blocked after all the CNG channels are constitutively opened.

To investigate whether cyclic nucleotides gate a conductance in SCN-projecting RGCs, either 500 μM cAMP ($n = 5$) or 500 μM cGMP ($n = 6$) was included in the recording pipette during whole-cell voltage-clamp recordings. Baseline currents were monitored immediately upon break-in and for up to 90 min. Neither cAMP nor cGMP activated an inward current (Fig. 3A; cAMP, one-way ANOVA $P = 0.954$, $F = 0.212$; cGMP, one-way ANOVA $P = 0.836$, $F = 0.412$). We considered the possibility that endogenous phosphodiesterases would hydrolyse the 500 μM cAMP or 500 μM cGMP that was introduced to the cell via the pipette solution. To maximize the intracellular concentration of cyclic nucleotides, we applied 500 μM 3-isobutyl-1-methylxanthine (IBMX), a broad-spectrum phosphodiesterase inhibitor, via the bath to the 11 cells represented in Fig. 3. The timing of IBMX application was different for each cell, and so it is not indicated in Fig. 3A. IBMX in combination with cAMP or cGMP had no effect on baseline membrane currents. Two representative cells are shown in Fig. 3B and C.

Although inclusion of cyclic nucleotides in the intracellular solution did not directly activate any currents in SCN-projecting RGCs, cyclic nucleotides are known to activate a number of enzymes that can modulate signaling cascades and ion channels. Therefore, we next addressed whether light responses were modulated by intracellular cyclic nucleotides. Light responses were evoked every 4 min during whole-cell voltage-clamp recordings with either 500 μM cAMP or cGMP in the recording pipette. Bath-applied IBMX (500 μM) was used to further increase the intracellular concentration of cyclic nucleotides. To distinguish between pharmacological block and rundown, IBMX was applied only after the light responses of each cell reached a steady-state amplitude. Light responses could still be elicited after intracellular perfusion of cAMP and cGMP and 15 min of IBMX application (Fig. 3B and C, respectively). The persistence of the light response despite high internal concentrations of cyclic nucleotides indicates that a molecule other than cAMP or cGMP is gating the light-activated channel. However, cyclic nucleotides did modulate the amplitude of the light response. In five cells with pipette solutions containing cAMP, bath application of IBMX reduced the light response by 23.0 ± 4% (Fig. 3D, left; Student's paired *t*-test, $P < 0.002$). Similarly, IBMX reduced the light response by 37.8 ± 5% in five cells containing cGMP (Fig. 3C, right; Student's paired *t*-test, $P < 0.012$). In eight of ten cells, the effect of IBMX was reversible following washout ($n = 5$ cGMP, $n = 3$ cAMP).

To rule out further a role for CNG channels in the intrinsic light response, we applied a cocktail of known blockers of CNG channels during light stimulation of SCN-projecting RGCs. Light responses evoked in whole-cell voltage-clamp conditions were compared before and after the application of CNG channel blockers. The light response was unaffected (data not shown) when the CNG channel blocker pimozide (50 μM, Student's paired *t*-test, $P = 0.18$) was applied to five cells in whole-cell voltage-clamp mode. Additionally, when a cocktail containing pimozide (50 μM) l-*cis*-diltiazem (30 μM), and dichlorobenzamil (30 μM) was applied to three cells in whole-cell voltage-clamp mode, and two cells in perforated-patch current-clamp mode, neither the light-activated current nor the light-activated depolarization, respectively, were blocked (Nicol *et al.*, 1987; Haynes, 1992; Nicol, 1993).

## Role of divalent ions

The conductance of CNG channels is dramatically reduced by the presence of divalent cations, which act as voltage-dependent permeant blockers (Haynes, 1995; Zimmerman & Baylor, 1992; Kleene, 1995).
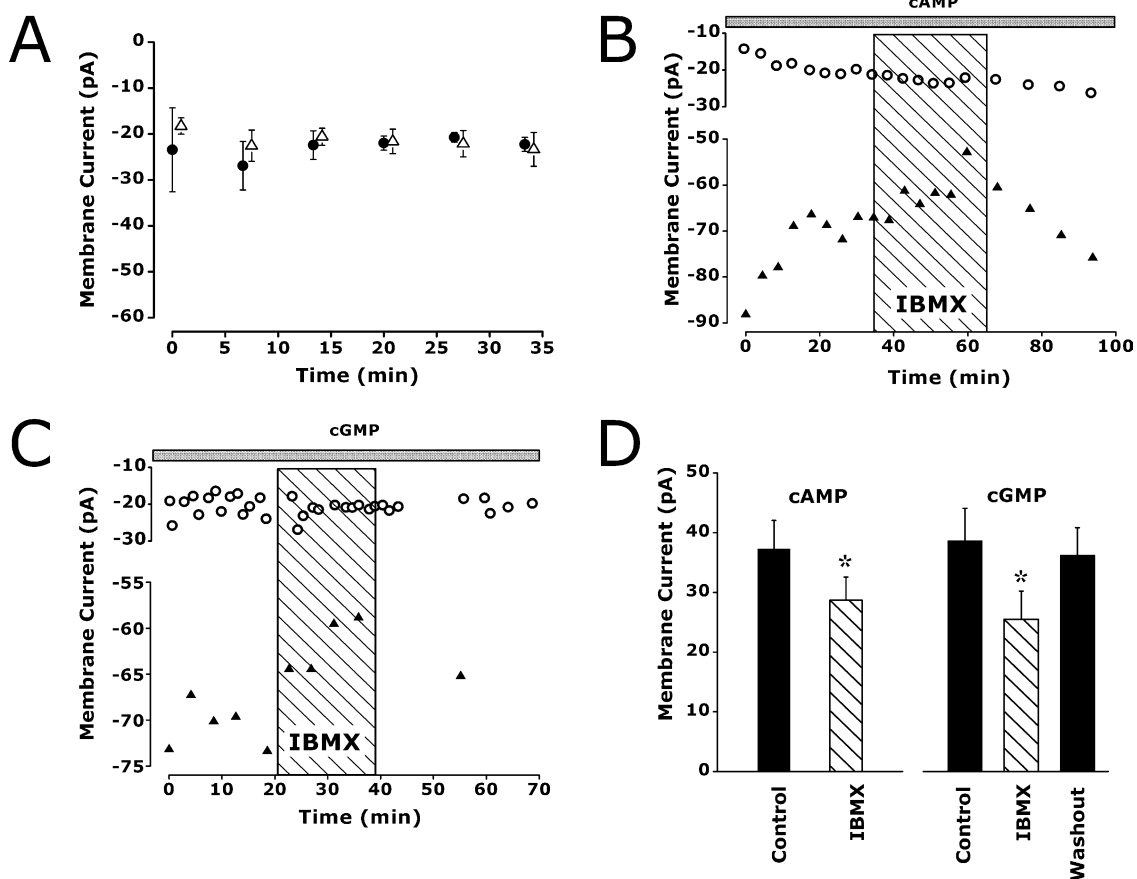
FIG. 3. Cyclic nucleotides modulate the light response but do not gate the light-activated channel. (A) Average whole-cell baseline currents were plotted from cells with pipette solutions containing either 500 μM cAMP (●) or 500 μM cGMP (△). One-way ANOVA detected no significant change in baseline currents of either population over the 33 min recording period. (B and C) Baseline currents (○) and peak light-activated currents (▲) from two SCN-projecting RGCs with pipette solutions containing either 500 μM cAMP (B) or 500 μM cGMP (C): 500 μM IBMX application is represented by hatched box. (D) Coapplication of IBMX with cAMP or with cGMP significantly reduced the light response. *Significantly different from control ($P < 0.002$ with cAMP and $P < 0.012$ with cGMP).

At negative potentials, extracellular divalents are particularly effective at reducing the inward cation current. Therefore, if the intrinsic light response were mediated by CNG channels, removal of extracellular divalents would be expected to enhance the light response dramatically between 20- and 500-fold, depending upon the CNG channel isoform (Haynes, 1995; Zimmerman & Baylor, 1992; Kleene, 1995). Although removal of extracellular divalents caused the recordings to become unstable, there was no marked increase in the magnitude of the light response (data not shown).

Intracellular divalent cations have also been shown to reduce the conductance of CNG channels, although their effects would be moderate at a holding potential of −60 mV. Intracellular calcium is known to modulate the affinity of CNG channels in a calmodulin-dependent manner (Hsu & Molday, 1993; Molday, 1996; Bradley et al., 2005). Therefore, we compared the amplitude of the light response and the time to peak in the presence of increasing amounts of divalent buffering: 0.1 mM EGTA, 10 mM EGTA and 18 mM BAPTA. The intracellular concentrations of free $Mg^{2+}$ and Mg-ATP were estimated using the web-based Max Chelator program (http://www.stanford.edu/~cpatton/webmaxc/webmaxcS.htm), and were found to change only moderately, within a range of 0.83–1.27 mM for free $Mg^{2+}$, and 3.58–3.88 mM for Mg-ATP. From these estimations, we conclude that the effects seen in Fig. 4A and B are due primarily to differences in calcium buffering.

As shown in Fig. 4A (upper), light responses evoked in whole-cell voltage-clamp from cells containing 10 mM EGTA had an average

amplitude of −72.6 ± 9.2 pA ($n = 7$). In the presence of 18 mM intracellular BAPTA, the amplitude of the light response was significantly reduced by 69% to −22.5 ± 4.0 pA ($n = 4$; one-way ANOVA, $P < 0.004$) when compared with light responses evoked in 10 mM EGTA. In weakly buffered solutions containing 0.1 mM EGTA, the amplitude of the light response was only slightly reduced (63.3 ± 6.7 pA, $n = 7$; one-way ANOVA, $P > 0.42$) when compared with light responses evoked in 10 mM EGTA. The degree of calcium buffering also altered the kinetics of the intrinsic light response. In the presence of 0.1 mM EGTA, the light response peaked after a delay of 2.9 ± 0.3 s ($n = 7$); in the presence of 18 mM BAPTA, the light response peaked only after a delay of 6.2 ± 2 s (Fig. 4A, lower; $n = 4$). This was significantly slower than the average time to peak measured in cells containing 0.1 mM EGTA (one-way ANOVA, $P < 0.025$).

In addition to its effect on light response amplitude and rate, increased calcium buffering also reduced the rate of light-activated current rundown. In Fig. 4B (upper), the normalized light responses from cells in 0.1 and 10 mM EGTA are plotted and fit with single exponentials. The average time constant (Fig. 4B, lower) of rundown in 0.1 mM EGTA ($n = 6$) was 212 ± 75 s, which was significantly shorter ($P = 0.05$ Student's t-test) than that in 10 mM EGTA ($n = 6$, $\tau = 592 ± 150$ s). In cells containing 18 mM BAPTA ($n = 4$), rundown did not fit a single exponential decay. Three of the four cells in which BAPTA was used as a buffer showed small initial light responses that dropped to even smaller steady-state amplitudes
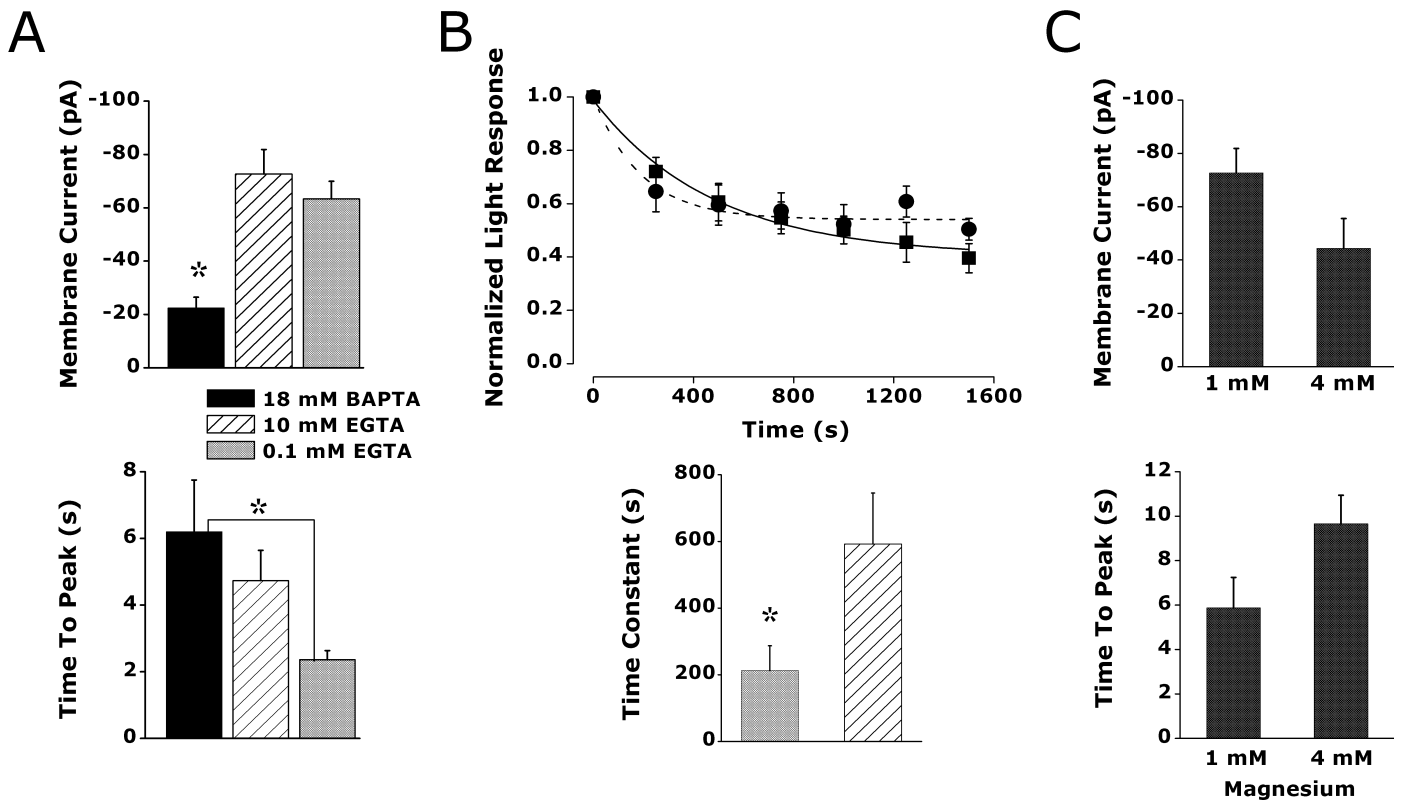
FIG. 4. Divalent ions modulate the light-activated current. (A) Upper: the average light response amplitude is significantly smaller when 18 mM BAPTA (black) is included in the pipette compared with 10 mM EGTA (hatched) and 0.1 mM (grey). Lower: the rate of the response is significantly longer in 18 mM BAPTA than in 0.1 mM EGTA. (B) Upper: light responses were normalized to the first maximal light response and the averages for each group plotted over 1600 s. Both cells with 0.1 mM EGTA (●) and cells with 10 mM EGTA (■) in the pipette solution reached a steady-state light response amplitude around 50% of initial amplitude. Lower: the time constants of rundown were calculated by fitting data from each cell to a single exponential decay and averaging within a group. (C) Upper: increasing internal magnesium from 1 mM to 4 mM reduced the amplitude of the light response. Lower: the increase in magnesium also slowed the development of the light-activated inward current. Neither of these findings were significant by Student's *t*-test. Asterisks indicate: $P < 0.004$ compared with 10 mM EGTA in A upper panel; $P < 0.025$ in A lower panel; $P = 0.05$ in panel B.

immediately. The fourth cell showed a steady linear decay in amplitude. Because cells containing 10 mM EGTA responded with maximal amplitudes, faster times to peak, and finally minimal rundown, 10 mM EGTA became the standard pipette solution buffer for all subsequent experiments.

To assess the role of internal magnesium in modulating the light-activated current (Fig. 4C), the concentration of intracellular $Mg^{2+}$ was changed while the divalent buffering was kept constant (10 mM EGTA). Although the differences in light response amplitude ($P = 0.078$) and time to peak ($P = 0.081$) were not statistically significant between cells containing 1 mM $MgCl_2$ ($n = 7$) and 4 mM $MgCl_2$ ($n = 5$), a trend emerged in which higher $Mg^{2+}$ reduced the amplitude and slowed the light response.

### Potential role of TRP channels

TRP channels were considered as possible candidates for the light-activated channel because TRP and TRP-like channels mediate a depolarizing light response in *Drosophila* photoreceptors. We first determined if ruthenium red (RR), a potent ryanodine receptor antagonist that also blocks TRPV and TRPC channels, inhibited the light response. In whole-cell voltage-clamp and perforated-patch current-clamp recordings, application of 20 μM RR reduced the intrinsic light response by $94 \pm 1\%$ ($n = 3$) and $86 \pm 12\%$ ($n = 3$), respectively (Fig. 5A). SK&F 96365 has been reported to be an effective blocker of TRP channels in a number of heterologous

expression systems (Boulay *et al.*, 1997; Zhu *et al.*, 1998; Inoue *et al.*, 2001; Riccio *et al.*, 2002). In whole-cell voltage-clamp mode at a holding potential of −60 mV addition of 200 μM SK&F 96365 to the bathing media significantly reduced the size of the light-activated current by $48.4 \pm 22\%$ ($n = 8$; Student's paired *t*-test, $P = 0.005$; Fig. 5B).

The nonselective cation channel blockers lanthanum and gadolinium are widely reported to block TRP channels. Both were bath applied to SCN-projecting RGCs to determine their effects on the light-activated current. Lanthanum effectively blocked the light response at 100 μM in perforated-patch current-clamp recordings ($n = 2$, Fig. 5C), and reduced the light response amplitude at 500 μM in whole-cell voltage-clamp recordings by $60 \pm 17\%$ ($n = 3$). Gadolinium (200 μM) also reduced the amplitude of the light-activated current by $72.9 \pm 8\%$ in whole-cell voltage-clamp recordings ($n = 3$, Fig. 5D).

Because of the similarity between the *I–V* curve of the light-activated current and those published for currents through TRPC6 channels and other members of the TRPC3/6/7 family (Hofmann *et al.*, 1999; Okada *et al.*, 1999; Jung *et al.*, 2002; Warren *et al.*, 2003), we tested pharmacological agents known to target those channels. The nonselective cation channel blocker flufenamic acid is useful for distinguishing channels within the TRPC3/6/7 subfamily, as it blocks currents through TRPC3 and TRPC7 channels and potentiates currents through TRPC6 channels (Inoue *et al.*, 2001). Bath application of 250 μM flufenamic acid to SCN-projecting RGCs in the perforated-
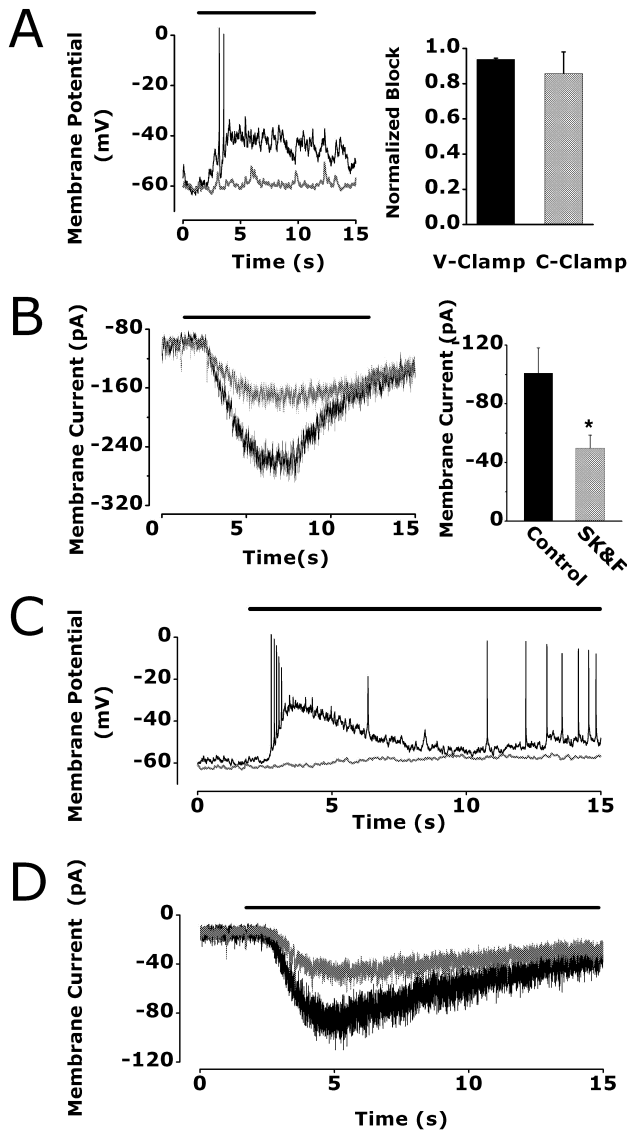
FIG. 5. TRP channel antagonists block the intrinsic light response. (A) Left: 20 μM ruthenium red blocked the intrinsic light response in an SCN-projecting RGC during a perforated-patch current clamp recording. Right: summary data showing percentage block by ruthenium red in three whole-cell voltage-clamp (black) and three perforated-patch current-clamp recordings (grey). (B) SK&F (200 μM), a TRPC channel blocker, significantly reduced the amplitude of the light-activated current by 48.4% ± 22 (*n* = 8). (C) LaCl$_3$ (100 μM) blocked the intrinsic light response in a perforated-patch current-clamp recording. (D) GdCl$_3$ (200 μM) reduced the whole-cell light-activated current in this SCN-projecting RGC by 57%. Black traces in A–D represent control data and light stimulation is represented by black bars. *$P < 0.005$.
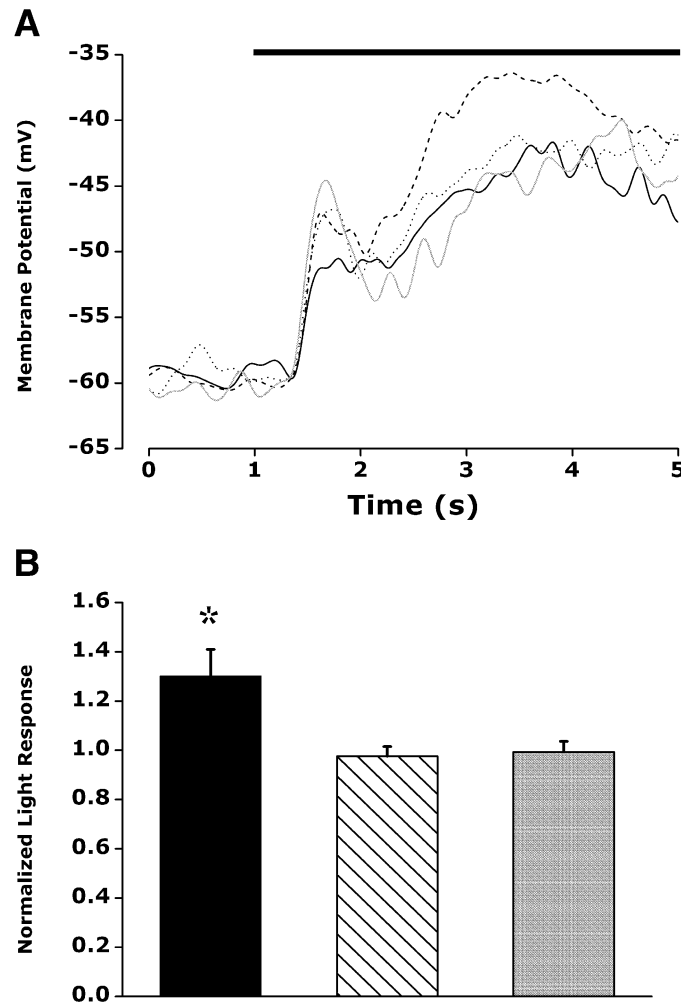


FIG. 6. 1-Oleoyl-2-acetyl-*sn*-glycerol (OAG) potentiated the intrinsic light response in a PKC-dependent manner. (A) Data taken from one SCN-projecting neuron, low-pass filtered at 2 Hz. In order of applications: control, black; 20 μM sphingosine, dotted; 100 μM OAG, dashed; OAG and sphingosine, grey. (B) OAG (100 μM) significantly potentiated the intrinsic light response in 18 SCN-projecting RGCs during perforated-patch current-clamp recordings (black). The PKC antagonist sphingosine (20 μM) had no effect on the light response when applied alone to five cells (hatched). Coapplication of OAG and sphingosine blocked the OAG-induced potentiation (*n* = 4, grey). *$P = 0.008$.

patch configuration did not block the light response, but caused a 9.9 ± 4% increase in the light-activated depolarization (*n* = 3, data not shown).

We then studied the effects of the TRPC3/6/7 channel activator 1-oleoyl-2-acetyl-*sn*-glycerol (OAG) on the intrinsic light response. OAG, a membrane-permeant analog of diacylglycerol, was applied at 100 μM to 18 SCN-projecting neurons during perforated-patch current-clamp recordings. While OAG did not induce a depolarization in the absence of light stimulation, it did significantly potentiate the peak of the light-activated depolarization by 28.4 ± 10% ($P = 0.008$

paired Student's *t*-test, Fig. 6B). One downstream effect of diacylglycerol is stimulation of protein kinase C (PKC). To determine if the potentiating effect of OAG on the intrinsic light response was mediated through PKC, we applied the PKC antagonist sphingosine (20 μM) (Hannun *et al*., 1991). When applied alone, sphingosine had no effect on the light-induced depolarization (*n* = 5). When coapplied with OAG, sphingosine blocked OAG-induced potentiation (*n* = 4), suggesting that OAG enhanced the light-activated current via activation of PKC.

### Immunohistochemistry

Immunohistochemistry was used to investigate the possible expression of CNG and TRPC6 channels in melanopsin-containing RGCs. As shown in Fig. 7A, although there was robust staining of CNGA1 and CNGA3 in rod and cone photoreceptors, respectively, we saw no evidence for expression of any CNG channel isoforms in melanopsin-
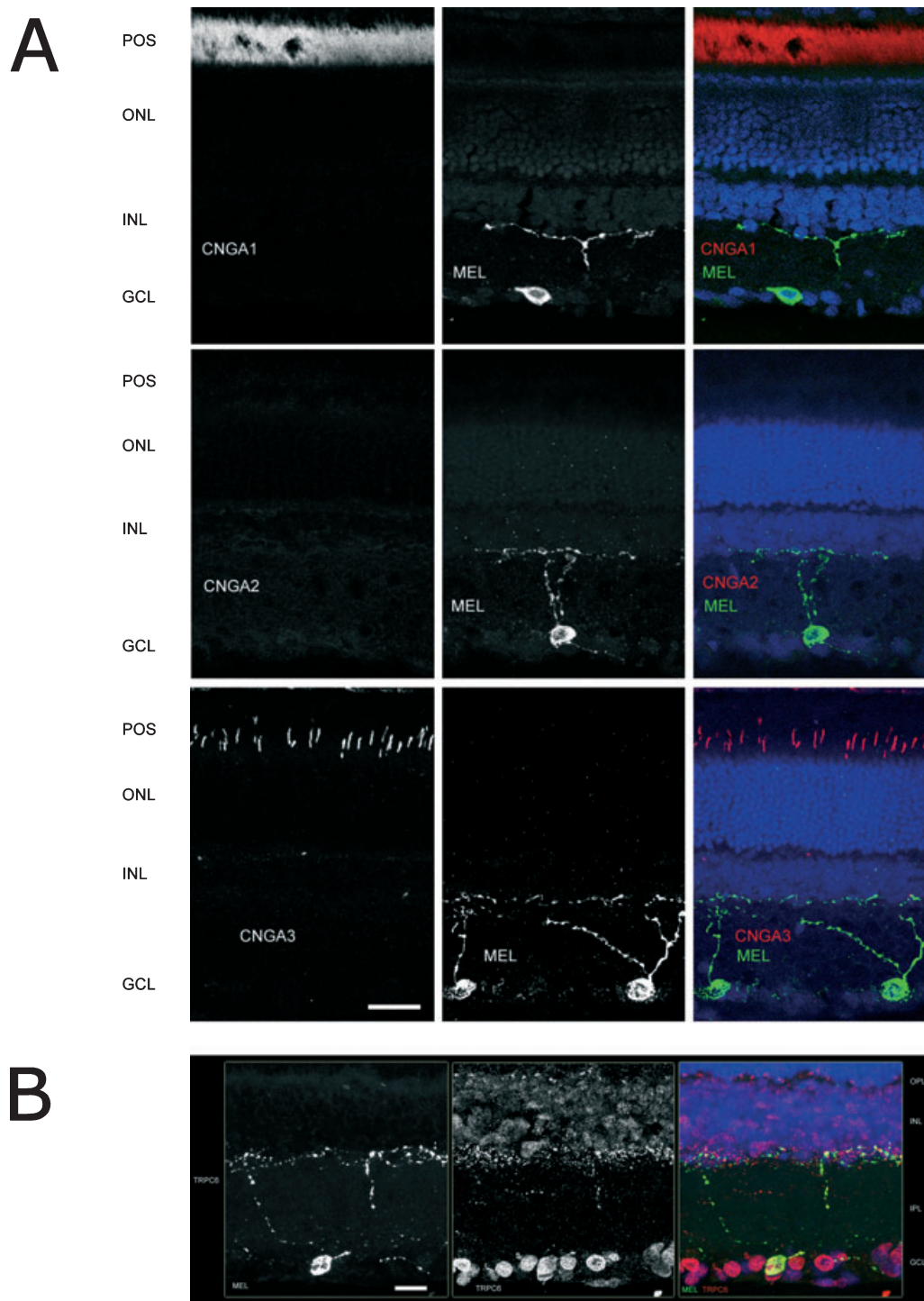
FIG. 7. Ion channel expression in melanopsin-containing RGCs. (A) CNG channels do not colocalize with melanopsin. Retinal sections were immunostained for melanopsin (green) and CNGA1 (top, red), CNGA2 (middle, red) and CNGA3 (bottom, red). DAPI-staining of cell nuclei (blue) was used to visualize retinal layers. (B) TRPC6 channels are found in most RGCs, including those that express melanopsin. Melanopsin (green) was visualized by tyramide signal amplification, and TRPC6 (red) was visualized using conventional immunostaining techniques (see Methods). Scale bars, 20 μm. Abbreviations: POS (photoreceptor outer segments); ONL (outer nuclear layer); OPL (outer plexiform layer); INL (inner nuclear layer); IPL (inner plexiform layer); GCL (ganglion cell layer).

containing RGCs. The olfactory isoform was not detected anywhere in the retina. By contrast, as shown in Fig. 7B, TRPC6 was expressed in most cells in the RGC layer, including those that contained melanopsin. There was also punctuate TRPC6 labeling in processes in the outermost layer of the inner plexiform layer, some of which was coincident with melanopsin. TRPC6 expression was also prominent in the outer plexiform layer, and was present at lower levels in cells of the inner nuclear layer. Several control experiments confirmed the colocalization was not due to the Alexa594-labeled secondary antibody cross-reacting with the α-melanopsin IgG: first, no labeling was seen when the α-TRPC6 antibody was omitted from the second round of staining; and, second, no colocalization was seen when using

the TSA technique with antibodies against melanopsin and PKC-α, which is confined to rod bipolar cells (data not shown).

## Discussion

Our previous work characterized the intrinsic light response of SCN-projecting RGCs in whole-cell patch-clamp recordings (Warren *et al.*, 2003). In the present study, we use pharmacology to investigate the identity of the light-activated channel and the underlying intracellular signaling pathway leading to its activation.

Approximately 80–90% of SCN-projecting RGCs express melanopsin (Gooley *et al.*, 2001; Morin *et al.*, 2003; Sollars *et al.*, 2003), a novel invertebrate-like opsin first described in *Xenopus* dermal melanophores (Provencio *et al.*, 1998) and found in the inner nuclear and ganglion cell layers of retina (Provencio *et al.*, 2000). Its predicted structure is that of a seven transmembrane G-protein-coupled receptor (Provencio *et al.*, 1998). Melanophores respond to light by dispersing pigment granules in a PLC/PKC/calcium-dependent manner (Isoldi *et al.*, 2005). In heterologous expression systems, melanopsin forms a functional G-protein-coupled photopigment that can activate a TRPC3 current in response to light (Panda *et al.*, 2005; Qiu *et al.*, 2005). Melanopsin has also been shown to couple effectively to other G-proteins (Newman *et al.*, 2003) and unidentified endogenous ion channels in the mouse Neuro-2A cell line (Melyan *et al.*, 2005). In the present study we establish an essential role for G-proteins in generating the intrinsic light response of SCN-projecting RGCs by demonstrating that stimulatory and inhibitory analogs of GTP abolish the light-activated current. The G-protein dependence of the light-activated pathway is consistent with that of melanopsin-based signal transduction reported in other systems.

### CNG channels do not mediate the light-activated current

Several lines of evidence suggest that CNG channels do not mediate the intrinsic light response in SCN-projecting RGCs. First, inclusion of cAMP and cGMP in the intracellular pipette solution at a concentration at least 20-fold greater than the $K_{1/2}$ did not activate inward currents or completely block the light response, even after coapplication of IBMX (Fesenko *et al.*, 1985; Kaupp & Seifert, 2002). Second, bath application of CNG channel antagonists did not block the light response. Pimozide is a voltage-independent blocker of rod CNG channels with a $K_{1/2}$ of ∼ 1 μM (Nicol, 1993), and would be expected to eliminate > 95% of rod channel current at the concentration used in this study. Dichlorobenzamil is a potent inhibitor of both the rod and the olfactory CNG channels ($K_{1/2}$ of ∼ 1 and 4 μM, respectively) and should block 90–95% of CNG current under the conditions used in this study (Nicol *et al.*, 1987; Kolesnikov & Kosolapov, 1993). L-*cis*-diltiazem is a potent inhibitor of all three isoforms of CNG channel with $K_{1/2}$ values of 2.6, 47 and 49 μM at −30 mV for the rod, olfactory and cone channels, respectively (Haynes, 1992; Kolesnikov *et al.*, 1990). Third, immunohistochemistry shows no evidence for any CNG channel isoforms in melanopsin-containing RGCs. Finally, as discussed below, the effects of divalent cations and intracellular calcium buffering on the light response are not consistent with a role for CNG channels in the intrinsic light response.

### Sensitivity of the light-activated current to cations

Extracellular divalent cations function as voltage-dependent permeant blockers of CNG channels by impeding the passage of monovalent cations. In the presence of physiological concentrations of $Ca^{2+}$ and $Mg^{2+}$, the conductance of CNG channels is dramatically reduced (Zufall & Firestein, 1993; Haynes, 1995; Kleene, 1995). For example, at a holding potential of −60 mV, the conductance of the retinal rod is most profoundly affected, being reduced from 24 pS in the absence of divalent cations to < 0.1 pS under physiological conditions (Gray & Attwell, 1985). However, the intrinsic light response in SCN-projecting RGCs persists in external solutions containing 3 mM $Ca^{2+}$ and 1 mM $Mg^{2+}$, sometimes attaining a magnitude of 100 pA, which is several times larger than the photoresponse of retinal rods.

Although the light response was not blocked by external or internal divalent ions, intracellular calcium and magnesium levels seemed to modulate both the amplitude and the kinetics of the light-activated current. Addition of 18 mM BAPTA to the pipette solution caused a dramatic reduction in the amplitude of the light response, compared with that seen in 0.1 and 10 mM EGTA. Again, this behaviour is inconsistent with the known behaviour of CNG channels. For all native CNG channels, the cyclic nucleotide sensitivity is reduced by binding of the $Ca^{2+}$-calmodulin complex, although this effect is most pronounced in the olfactory channel (Hsu & Molday, 1993; Wei *et al.*, 1998). Therefore, in contrast to our experimental findings, we would predict that increased buffering of intracellular $Ca^{2+}$ would enhance the light response if it were mediated by CNG channels.

### Evidence that TRP channels mediate the light-activated current

The TRP superfamily is composed of three families of ion channels (TRPC, TRPV, TRPM) whose members share sequence homology with TRP and TRP-like channels first described in the *Drosophila* photoreceptor. We considered members of the TRPC family specifically because they have the most sequence homology with *Drosophila* TRP channels and are widely expressed in mammalian nervous systems. Indeed, our immunocytochemical experiments clearly show that TRPC6 channels are expressed in many RGCs, including those that express melanopsin, in addition to other neurons in the inner nuclear layer and outer plexiform layer. The physiological role of TRPC6 channels in these neurons is unknown. However, depending on the nature of the upstream second messenger pathway, this role could vary quite markedly from one cell type to another. While TRPC channel gating depends on the particular cell type in which a channel is expressed, all TRP channel proteins lie downstream of $G_q$ and PLC activation. TRP channel activators include calcium store depletion and products of PLC activation (Hofmann *et al.*, 1999; Okada *et al.*, 1999; Inoue *et al.*, 2001; Minke & Cook, 2002).

Both cAMP and cGMP, in concert with IBMX, reduced the size of the inward current evoked by light, suggesting a role for the cyclic nucleotide-dependent kinases, PKA and PKG, in modulating the light-activated current. Consensus phosphorylation sites have been described for all seven TRP channel proteins, but the effects of phosphorylation by PKA and PKG have, to date, only been studied on TRPC3 and TRPC6 channels (Kwan *et al.*, 2004). Current through TRPC3 is inhibited by PKG activation, while currents through TRPC6 are unaffected after phosphorylation by either PKA or PKG (Hassock *et al.*, 2002; Kwan *et al.*, 2004).

The results from our pharmacological experiments also provide further support for the hypothesis that the light-activated current is mediated by a TRP channel. Although no compounds have been shown selectively to block TRP channels, the effects of many pharmacological agents on TRP channels are well established and consistent (Gosling *et al.*, 2005). The two types of channel blockers most commonly used to identify TRP channels are SK&F 96365, a

blocker of receptor-activated calcium entry, and the lanthanides gadolinium and lanthanum. SK&F 96365 was originally developed as a blocker of receptor-activated calcium current (Merritt *et al.*, 1990), and has been shown to block TRPC6 (Inoue *et al.*, 2001). In the current study SK&F 96365 blocks 48.4% of the light-activated current. Extracellular application of lanthanum (0.1–4.0 mM) (Zhu *et al.*, 1998; Halaszovich *et al.*, 2000) and gadolinium (150–200 μM) (Trebak *et al.*, 2002) block TRPC3 and TRPC6 channels and potentiate currents through TRPC4 and TRPC5 channels (Jung *et al.*, 2003). Our observations that these ions block the light-activated channel would seem to eliminate TRPC4 and TRPC5 as candidates. The high concentration required for lanthanide block in our study may reflect a site of action on the intracellular side of the light-activated channel, or it may be a feature of the specific subunit composition of channels in the native SCN-projecting RGC (Halaszovich *et al.*, 2000). Moreover, flufenamic acid did not inhibit the light response in SCN-projecting RGCs, suggesting that the light-activated channel is not a homomeric TRPC3 or TRPC7 channel, but may contain TRPC6 subunits (Inoue *et al.*, 2001).

Currents mediated by TRP channels exhibit a complex dependence on calcium much like we see for the light-activated current in SCN-projecting RGCs. Both their activation and their inactivation are modulated by a variety of calcium-dependent processes including internal store depletion, CaM binding and phosphorylation by calcium-dependent kinases, including both CaMKII and PKC. Binding sites for the IP$_3$ receptors and CaM exist on all seven TRPC proteins, and these domains interact in a calcium-dependent way to inhibit channel activity (Tang *et al.*, 2001). Considering the TRPC3/6/7 subfamily specifically, internal calcium (Ca$^{2+}_i$) differentially regulates TRPC6 and TRPC7. Resting levels of Ca$^{2+}_i$ (80 nM) are known to enhance the amplitude and kinetics of current through TRPC6 channels, but inhibit current through TRPC7 channels. Higher concentrations of Ca$^{2+}_i$ (2 mM) inhibit currents through both channel subtypes (Shi *et al.*, 2004). Although we cannot quantify the [Ca$^{2+}_i$] in SCN-projecting RGCs from which we recorded, our results indicate that some amount of Ca$^{2+}_i$ is required to elicit larger and faster intrinsic light responses. The dependence of the light response on Ca$^{2+}_i$ is consistent with the reported potentiation of TRPC6-mediated currents by Ca$^{2+}_i$.

Although much of our evidence points towards TRPC6 as the best candidate for the light-activated channel, the effects of OAG on the light response in SCN-projecting RGCs complicate this interpretation. OAG has been shown to gate TRPC3/6/7 channels directly (Hofmann *et al.*, 1999); however, it failed to gate a current in SCN-projecting RGCs. In addition, the block of OAG-induced potentiation by sphingosine suggests that OAG is modulating the light response via PKC activation. While TRP channels contain PKC binding sites near their C termini, PKC stimulation by OAG or phorbol ester has previously been reported to inactivate, rather than enhance, TRPC-mediated currents (Venkatachalam *et al.*, 2003; Trebak *et al.*, 2005).

In HEK 293 cells expressing TRPC6 channels, application of low concentrations of carbachol has been shown to potentiate submaximal OAG responses (Estacion *et al.*, 2004). The authors of this study concluded that the TRPC6 channels were being synergistically regulated by multiple signaling pathways, both of which need to be activated to elicit a maximal response. Our observation that OAG enhances the amplitude of the light response without itself stimulating a current is somewhat consistent with these findings if TRPC6 mediates the light-activated current. The effective concentration of OAG may be reduced in the retinal whole-mount preparation due to membrane sequestration leaving only a subthreshold concentration of OAG available at the site of action in SCN-projecting RGCs. Similar to receptor stimulation by carbachol in the TRPC6-expressing HEK cells, light stimulation of the SCN-projecting RGCs might enhance the effect of low concentrations of OAG by synergistic activation of convergent signaling pathways. Further research is required to resolve this confounding issue and confirm the hypothesis that TRPC6 channels mediate the light response in SCN-projecting RGCs.

## Closing remarks

From these studies, we conclude that the intrinsic light response in SCN-projecting RGCs lies downstream of a G-protein-mediated signaling cascade. We provide strong evidence against a role for CNG channels and strengthen the case for TRP channels by demonstrating that several pharmacological agents that target TRP channels block the intrinsic light response. Future studies will focus on the specific subtype of TRP channel(s) involved in the intrinsic light response.

## Abbreviations

CNG, cyclic nucleotide-gated; IBMX, 3-isobutyl-1-methylxanthine; OAG, 1-oleoyl-2-acetyl-*sn*-glycerol; PKC, protein kinase C; RGC, retinal ganglion cell; SCN, suprachiasmatic nuclei; TRP, transient receptor potential.

## References

Bandyopadhyay, B.C. & Payne, R. (2004) Variants of TRP ion channel mRNA present in horseshoe crab ventral eye and brain. *J. Neurochem.*, **91**, 825–835.

Baylor, D.A. (1987) Photoreceptor signals and vision. Proctor lecture. *Invest. Ophthalmol. Vis. Sci.*, **28**, 34–49.

Berson, D.M., Dunn, F.A. & Takao, M. (2002) Phototransduction by retinal ganglion cells that set the circadian clock. *Science*, **295**, 1070–1073.

Boulay, G., Zhu, X., Peyton, M., Jiang, M., Hurst, R., Stefani, E. & Birnbaumer, L. (1997) Cloning and expression of a novel mammalian homolog of Drosophila transient receptor potential (Trp) involved in calcium entry secondary to activation of receptors coupled by the Gq class of G protein. *J. Biol. Chem.*, **272**, 29672–29680.

Bradley, J., Reisert, J. & Frings, S. (2005) Regulation of cyclic nucleotide-gated channels. *Curr. Opin. Neurobiol.*, **15**, 343–349.

Estacion, M., Li, S., Sinkins, W.G., Gosling, M., Bahra, P., Poll, C., Westwick, J. & Schilling, W.P. (2004) Activation of human TRPC6 channels by receptor stimulation. *J. Biol. Chem.*, **279**, 22047–22056.

Fesenko, E.E., Kolesnikov, S.S. & Lyubarsky, A.L. (1985) Induction by cyclic GMP of cationic conductance in plasma membrane of retinal rod outer segment. *Nature*, **313**, 310–313.

Gooley, J.J., Lu, J., Chou, T.C., Scammell, T.E. & Saper, C.B. (2001) Melanopsin in cells of origin of the retinohypothalamic tract. *Nat. Neurosci.*, **4**, 1165–1169.

Gosling, M., Poll, C. & Li, S. (2005) TRP channels in airway smooth muscle as therapeutic targets. *Naunyn Schmiedebergs Arch. Pharmacol.*, **371**, 277–284.

Gray, P. & Attwell, D. (1985) Kinetics of light-sensitive channels in vertebrate photoreceptors. *Proc. R. Soc. Lond. B Biol. Sci.*, **223**, 379–388.

Halaszovich, C.R., Zitt, C., Jungling, E. & Luckhoff, A. (2000) Inhibition of TRP3 channels by lanthanides. Block from the cytosolic side of the plasma membrane. *J. Biol. Chem.*, **275**, 37423–37428.

Hannun, Y.A., Merrill, A.H. Jr & Bell, R.M. (1991) Use of sphingosine as inhibitor of protein kinase C. *Meth. Enzymol.*, **201**, 316–328.

Hardie, R.C. (2001) Phototransduction in *Drosophila melanogaster*. *J. Exp. Biol.*, **204**, 3403–3409.

Hardie, R.C. & Minke, B. (1992) The trp gene is essential for a light-activated Ca$^{2+}$ channel in Drosophila photoreceptors. *Neuron*, **8**, 643–651.

Hassock, S.R., Zhu, M.X., Trost, C., Flockerzi, V. & Authi, K.S. (2002) Expression and role of TRPC proteins in human platelets: evidence that TRPC6 forms the store-independent calcium entry channel. *Blood*, **100**, 2801–2811.

Hattar, S., Liao, H.W., Takao, M., Berson, D.M. & Yau, K.W. (2002) Melanopsin-containing retinal ganglion cells: architecture, projections, and intrinsic photosensitivity. *Science*, **295**, 1065–1070.

Haynes, L.W. (1992) Block of the cyclic GMP-gated channel of vertebrate rod and cone photoreceptors by 1-cis-diltiazem. *J. Gen. Physiol.*, **100**, 783–801.

Haynes, L.W. (1995) Permeation and block by internal and external divalent cations of the catfish cone photoreceptor cGMP-gated channel. *J. Gen. Physiol.*, **106**, 507–523.

Hofmann, T., Obukhov, A.G., Schaefer, M., Harteneck, C., Gudermann, T. & Schultz, G. (1999) Direct activation of human TRPC6 and TRPC3 channels by diacylglycerol. *Nature*, **397**, 259–263.

Hsu, Y.T. & Molday, R.S. (1993) Modulation of the cGMP-gated channel of rod photoreceptor cells by calmodulin. *Nature*, **361**, 76–79.

Inoue, R., Okada, T., Onoue, H., Hara, Y., Shimizu, S., Naitoh, S., Ito, Y. & Mori, Y. (2001) The transient receptor potential protein homologue TRP6 is the essential component of vascular alpha (1) -adrenoceptor-activated Ca(2+)-permeable cation channel. *Circ. Res.*, **88**, 325–332.

Isoldi, M.C., Rollag, M.D., Lauro Castrucci, A.M. & Provencio, I. (2005) Rhabdomeric phototransduction initiated by the vertebrate photopigment melanopsin. *Proc. Natl Acad. Sci. USA*, **102**, 1217–1221.

Jung, S., Muhle, A., Schaefer, M., Strotmann, R., Schultz, G. & Plant, T.D. (2003) Lanthanides potentiate TRPC5 currents by an action at extracellular sites close to the pore mouth. *J. Biol. Chem.*, **278**, 3562–3571.

Jung, S., Strotmann, R., Schultz, G. & Plant, T.D. (2002) TRPC6 is a candidate channel involved in receptor-stimulated cation currents in A7r5 smooth muscle cells. *Am. J. Physiol. Cell Physiol.*, **282**, C347–C359.

Kaupp, U.B. & Seifert, R. (2002) Cyclic nucleotide-gated ion channels. *Physiol. Rev.*, **82**, 769–824.

Kleene, S.J. (1995) Block by external calcium and magnesium of the cyclic-nucleotide-activated current in olfactory cilia. *Neuroscience*, **66**, 1001–1008.

Kolesnikov, S.S. & Kosolapov, A.V. (1993) Cyclic nucleotide-activated channels in carp olfactory receptor cells. *Biochim. Biophys. Acta.*, **1150**, 63–72.

Kolesnikov, S.S., Zhainazarov, A.B. & Kosolapov, A.V. (1990) Cyclic nucleotide-activated channels in the frog olfactory receptor plasma membrane. *FEBS Lett.*, **266**, 96–98.

Kwan, H.Y., Huang, Y. & Yao, X. (2004) Regulation of canonical transient receptor potential isoform 3 (TRPC3) channel by protein kinase G. *Proc. Natl Acad. Sci. USA*, **101**, 2625–2630.

McNaughton, P.A. (1990) Light response of vertebrate photoreceptors. *Physiol. Rev.*, **70**, 847–883.

Melyan, Z., Tarttelin, E.E., Bellingham, J., Lucas, R.J. & Hankins, M.W. (2005) Addition of human melanopsin renders mammalian cells photo-responsive. *Nature*, **433**, 741–745.

Merritt, J.E., Armstrong, W.P., Benham, C.D., Hallam, T.J., Jacob, R., Jaxa-Chamiec, A., Leigh, B.K., McCarthy, S.A., Moores, K.E. & Rink, T.J. (1990) SK&F 96365, a novel inhibitor of receptor-mediated calcium entry. *Biochem. J.*, **271**, 515–522.

Meyer, M.R., Angele, A., Kremmer, E., Kaupp, U.B. & Muller, F. (2000) A cGMP-signaling pathway in a subset of olfactory sensory neurons. *Proc. Natl Acad. Sci. USA*, **97**, 10595–10600.

Minke, B. & Cook, B. (2002) TRP channel proteins and signal transduction. *Physiol. Rev.*, **82**, 429–472.

Molday, R.S. (1996) Calmodulin regulation of cyclic-nucleotide-gated channels. *Curr. Opin. Neurobiol.*, **6**, 445–452.

Montell, C. (2003) The venerable inveterate invertebrate TRP channels. *Cell Calcium*, **33**, 409–417.

Moore, R.Y. (1983) Organization and function of a central nervous system circadian oscillator: the suprachiasmatic hypothalamic nucleus. *Fed. Proc.*, **42**, 2783–2789.

Moore, R.Y. & Eichler, V.B. (1972) Loss of a circadian adrenal corticosterone rhythm following suprachiasmatic lesions in the rat. *Brain Res.*, **42**, 201–206.

Moore, R.Y., Speh, J.C. & Card, J.P. (1995) The retinohypothalamic tract originates from a distinct subset of retinal ganglion cells. *J. Comp. Neurol.*, **352**, 351–366.

Morin, L.P., Blanchard, J.H. & Provencio, I. (2003) Retinal ganglion cell projections to the hamster suprachiasmatic nucleus, intergeniculate leaflet, and visual midbrain: bifurcation and melanopsin immunoreactivity. *J. Comp. Neurol.*, **465**, 401–416.

Newman, L.A., Walker, M.T., Brown, R.L., Cronin, T.W. & Robinson, P.R. (2003) Melanopsin forms a functional short-wavelength photopigment. *Biochemistry*, **42**, 12734–12738.

Nicol, G.D. (1993) The calcium channel antagonist, pimozide, blocks the cyclic GMP-activated current in rod photoreceptors. *J. Pharmacol. Exp. Ther.*, **265**, 626–632.

Nicol, G.D., Schnetkamp, P.P., Saimi, Y., Cragoe, E.J Jr & Bownds, M.D. (1987) A derivative of amiloride blocks both the light-regulated and cyclic GMP-regulated conductances in rod photoreceptors. *J. Gen. Physiol.*, **90**, 651–669.

Okada, T., Inoue, R., Yamazaki, K., Maeda, A., Kurosaki, T., Yamakuni, T., Tanaka, I., Shimizu, S., Ikenaka, K., Imoto, K. & Mori, Y. (1999) Molecular and functional characterization of a novel mouse transient receptor potential protein homologue TRP7. Ca(2+)-permeable cation channel that is consti-tutively activated and enhanced by stimulation of G protein-coupled receptor. *J. Biol. Chem.*, **274**, 27359–27370.

Panda, S., Nayak, S.K., Campo, B., Walker, J.R., Hogenesch, J.B. & Jegla, T. (2005) Illumination of the melanopsin signaling pathway. *Science*, **307**, 600–604.

Provencio, I., Jiang, G., De Grip, W.J., Hayes, W.P. & Rollag, M.D. (1998) Melanopsin: an opsin in melanophores, brain, and eye. *Proc. Natl Acad. Sci. USA*, **95**, 340–345.

Provencio, I., Rodriguez, I.R., Jiang, G., Hayes, W.P., Moreira, E.F. & Rollag, M.D. (2000) A novel human opsin in the inner retina. *J. Neurosci.*, **20**, 600–605.

Qiu, X., Kumbalasiri, T., Carlson, S.M., Wong, K.Y., Krishna, V., Provencio, I. & Berson, D.M. (2005) Induction of photosensitivity by heterologous expression of melanopsin. *Nature*, **433**, 745–749.

Riccio, A., Mattei, C., Kelsell, R.E., Medhurst, A.D., Calver, A.R., Randall, A.D., Davis, J.B., Benham, C.D. & Pangalos, M.N. (2002) Cloning and functional expression of human short TRP7, a candidate protein for store-operated $Ca^{2+}$ influx. *J. Biol. Chem.*, **277**, 12302–12309.

Shi, J., Mori, E., Mori, Y., Mori, M., Li, J., Ito, Y. & Inoue, R. (2004) Multiple regulation by calcium of murine homologues of transient receptor potential proteins TRPC6 and TRPC7 expressed in HEK293 cells. *J. Physiol.*, **561**, 415–432.

Sollars, P.J., Smeraski, C.A., Kaufman, J.D., Ogilvie, M.D., Provencio, I. & Pickard, G.E. (2003) Melanopsin and non-melanopsin expressing retinal ganglion cells innervate the hypothalamic suprachiasmatic nucleus. *Vis. Neurosci.*, **20**, 601–610.

Tang, J., Lin, Y., Zhang, Z., Tikunova, S., Birnbaumer, L. & Zhu, M.X. (2001) Identification of common binding sites for calmodulin and inositol 1,4,5-trisphosphate receptors on the carboxyl termini of trp channels. *J. Biol. Chem.*, **276**, 21303–21310.

Trebak, M., Bird, G.S., McKay, R.R. & Putney, J.W. Jr (2002) Comparison of human TRPC3 channels in receptor-activated and store-operated modes. Differential sensitivity to channel blockers suggests fundamental differences in channel composition. *J. Biol. Chem.*, **277**, 21617–21623.

Trebak, M., Hempel, N., Wedel, B.J., Smyth, J.T., Bird, G.S. & Putney, J.W. Jr (2005) Negative regulation of TRPC3 channels by protein kinase C-mediated phosphorylation of serine 712. *Mol. Pharmacol.*, **67**, 558–563.

Venkatachalam, K., Zheng, F. & Gill, D.L. (2003) Regulation of canonical transient receptor potential (TRPC) channel function by diacylglycerol and protein kinase C. *J. Biol. Chem.*, **278**, 29031–29040.

Warren, E.J., Allen, C.N., Brown, R.L. & Robinson, D.W. (2003) Intrinsic light responses of retinal ganglion cells projecting to the circadian system. *Eur. J. Neurosci.*, **17**, 1727–1735.

Wassle, H., Grunert, U., Cook, N.J. & Molday, R.S. (1992) The cGMP-gated channel of rod outer segments is not localized in bipolar cells of the mammalian retina. *Neurosci. Lett.*, **134**, 199–202.

Wei, J.Y., Roy, D.S., Leconte, L. & Barnstable, C.J. (1998) Molecular and pharmacological analysis of cyclic nucleotide-gated channel function in the central nervous system. *Prog. Neurobiol.*, **56**, 37–64.

Zhu, X., Jiang, M. & Birnbaumer, L. (1998) Receptor-activated $Ca^{2+}$ influx via human Trp3 stably expressed in human embryonic kidney (HEK) 293 cells. Evidence for a non-capacitative $Ca^{2+}$ entry. *J. Biol. Chem.*, **273**, 133–142.

Zimmerman, A.L. & Baylor, D.A. (1992) Cation interactions within the cyclic GMP-activated channel of retinal rods from the tiger salamander. *J. Physiol.*, **449**, 759–783.

Zufall, F. & Firestein, S. (1993) Divalent cations block the cyclic nucleotide-gated channel of olfactory receptor neurons. *J. Neurophysiol.*, **69**, 1758–1768.